Front. Phys. 11(6), 117406 (2016)
DOI 10.1007/s11467-016-0578-1

RESEARCH ARTICLE

# Superconductivity well above room temperature in compressed $MgH_6$

**R. Szczęśniak**[1], **A. P. Durajski**[2,†]

[1] *Institute of Physics, Jan Długosz University, Ave. Armii Krajowej 13/15, 42-200 Częstochowa, Poland*
[2] *Institute of Physics, Częstochowa University of Technology, Ave. Armii Krajowej 19, 42-200 Częstochowa, Poland*
*Corresponding author. E-mail:* † *adurajski@wip.pcz.pl*
*Received March 8, 2016; Accepted March 26, 2016*

It has been suggested that hydrogen-rich systems at high pressure may exhibit notably high superconducting transition temperatures. One of the more interesting theoretical predictions was that hydrogen sulfide can be metallized and the high-temperature superconducting state can be induced. A record critical temperature (203 K) was later confirmed for $H_3S$ in an experiment. In this paper, we investigated, within the framework of the Eliashberg formalism, the properties of compressed $MgH_6$, which is expected to be a very good candidate for room-temperature superconductivity. This applies particularly to the pressure range from 300 to 400 GPa, where the transition temperature is close to 400 K. Moreover, the estimated thermodynamic properties and the resulting dimensionless ratios exceed the predictions of the Bardeen–Cooper–Schrieffer theory. This behavior is attributed to the strong electron–phonon coupling and retardation effects existing in hydrogen-dominated materials under high pressure.

**Keywords** superconductors, hydrogen-rich compounds, high pressure, thermodynamic properties

**PACS numbers** 74.20.Fg, 74.25.Bt, 74.62.Fj



## 1 Introduction

Following the pioneering work of Ashcroft, high-temperature superconductivity was predicted in compressed metallic molecular hydrogen [1]. Unfortunately, metallization of pristine hydrogen has proved to be extremely difficult because the required pressure is beyond the laboratory scale. Therefore, it was pointed out that because of chemical precompression in hydrogen-rich systems, the external pressure necessary for hydrogen metallization could be significantly decreased [2]. The latest results for superconductivity in pressurized hydrogen-rich compounds suggested that these materials have the potential to become very high-temperature superconductors [3]. Theoretical calculations [4–6] and experiments [7, 8] have found that the critical temperature ($T_C$) of sulfur hydride ($H_3S$) can be as high as 203 K at a pressure close to 150 GPa. This new record for phonon-mediated superconductivity has attracted much attention in terms of both theory and experiment. Currently, the most promising materials for room-temperature superconductors are sodalite-like calcium and magnesium hydrides ($CaH_6$ and $MgH_6$) at high pressure. For the former, the branch literature suggests that the critical temperature can reach a value close to 240 K at 150 GPa [9], whereas the latter is characterized by a record high $T_C$, which is estimated to be 263 K at 300 GPa [10]. In this paper, we focus on the theoretical description of the superconducting state in $MgH_6$ over a pressure range of 300–400 GPa.

## 2 Computational details

Optimizations and enthalpy calculations for compressed $MgH_6$ were performed previously [10] within density functional theory using the Vienna *ab initio* Simulation Package [11]. The generalized gradient approximation with the Perdew–Burke–Ernzerhof functional [12] for the exchange correlation was employed. The projector-augmented wave [13] method was adopted with valence electrons of $1s^1$ for H and $2s^2 2p^6 3s^2$ for Mg.

Calculations that aim at estimation of the thermodynamic properties of the superconducting state are conducted in the present paper within the framework of the Eliashberg formalism [14]. In the imaginary-axis formulation, the set of two nonlinear Eliashberg equations for the superconducting order parameter function $\Delta_n \equiv \Delta(\mathrm{i}\omega_n)$ and the mass renormalization function $Z_n \equiv Z(\mathrm{i}\omega_n)$ are given by [15]

$$\Delta_n Z_n = \frac{\pi}{\beta} \sum_{m=-M}^{M} \frac{K(\mathrm{i}\omega_n - \mathrm{i}\omega_m) - \mu^{\star}\theta(\omega_c - |\omega_m|)}{\sqrt{\omega_m^2 + \Delta_m^2}} \Delta_m \tag{1}$$

© Higher Education Press and Springer-Verlag Berlin Heidelberg 2016

and

$$Z_n = 1 + \frac{1}{\omega_n}\frac{\pi}{\beta}\sum_{m=-M}^{M}\frac{K\left(\mathrm{i}\omega_n - \mathrm{i}\omega_m\right)}{\sqrt{\omega_m^2 + \Delta_m^2}}\omega_m. \tag{2}$$

Here the Matsubara frequency is defined as $\omega_n \equiv (\pi/\beta)(2n-1)$, where $n = 0, \pm1, \pm2, \ldots, \pm M$, and $M = 1100$. The inverse temperature is given by $\beta \equiv 1/(k_B T)$, where $k_B$ represents the Boltzmann constant. The symbols $\theta$ and $\omega_c$ denote the Heaviside function and cutoff frequency, respectively. We found that the Eliashberg equations converged at $\omega_c = 10\Omega_{\max}$, where $\Omega_{\max}$ is the maximum phonon frequency. Further, $\mu^\star$ denotes the effective screened Coulomb repulsion constant, the value of which is generally chosen to be between 0.1 and 0.15. Recent theoretical investigations based on experimental data found that in hydrogen-rich compounds, $\mu^\star \approx 0.1$ [4, 16]. Therefore, we also adopted this value in the present studies. Moreover, the pairing kernel for the electron–phonon interaction that appears in Eqs. (1) and (2) is given by

$$K\left(\mathrm{i}\omega_n - \mathrm{i}\omega_m\right) \equiv 2\int_0^{\Omega_{\max}} \mathrm{d}\Omega \frac{\Omega}{\left(\omega_n - \omega_m\right)^2 + \Omega^2}\alpha^2 F\left(\Omega\right). \tag{3}$$

Our investigations are based on the Eliashberg spectral functions $\alpha^2 F(\Omega)$ determined in Ref. [10] by using the *ab initio* linear response method with a $4\times4\times4$ $q$-point mesh and $24\times24\times24$ $k$-point mesh for the first Brillouin zone integrations.

The validity of the Eliashberg theory and correctness of our numerical methods of describing the phonon-mediated superconducting state were confirmed on the basis of the experimental results in our previous papers, e.g., [17, 18].

## 3 Results and discussion

### 3.1 Critical temperature, energy gap, and electron effective mass

To calculate the physical values of the superconducting order parameter ($\Delta$) and electron effective mass ($m_e^\star$), the Eliashberg equations [Eqs. (1) and (2)] were solved, and the obtained results were analytically continued to the real frequency axis [15]. As shown in Fig. 1(a), at low temperatures, the order parameter reaches very high values; it gradually decreases with increasing temperature and finally vanishes at $T_c$. On the basis of these results, we conclude that $MgH_6$ is a candidate for superconductivity with $T_c$ well above room temperature. In particular, our calculations indicate that in this compound, the critical temperature decreases from 420 to 384 K when the pressure increases from 300 to 400 GPa.

For comparison, we collated the above results with the results obtained using the analytical Allen–Dynes [19] and McMillan formulas [20], as shown in Fig. 1(b). The very clear differences between the methods employed confirm that the superconducting state in pressurized $MgH_6$ cannot be properly described within the framework of the analytical approximations. The origin of this behavior is closely related to the strong electron–phonon coupling. The total electron–phonon coupling strength ($\lambda$) is estimated directly from the Eliashberg function:

$$\lambda = 2\int_0^\infty \frac{\alpha^2 F(\Omega)}{\Omega}\mathrm{d}\Omega. \tag{4}$$

Note that in the weak-coupling case [which is well described by the Bardeen–Cooper–Schrieffer (BCS) theory], the electron–phonon coupling constant is small ($\lambda \leq 0.5$). However, most superconducting materials exhibit intermediate ($\lambda$ on the order of 1) or strong electron–phonon coupling ($\lambda > 1$), and their superconducting properties are not well described by the BCS theory. For magnesium hydrides at high pressure, the evidence for strong electron–phonon coupling is presented in Ref. [10], in which the authors showed that in the investigated pressure range, $\lambda$ significantly exceeds 2. The strong correlations contribute to a significant renormalization of the electron effective mass. In our case, the ratio $m_e^\star/m_e$ (where $m_e$ denotes the electron band mass) decreases from 4.60 to 3.55 as the pressure increases from 300 to 400 GPa.

The computed values of the order parameter and critical temperature allowed us to determine the ratio of the universal zero-temperature energy gap [$2\Delta(0)$] to $T_c$: $R_\Delta = 2\Delta(0)/(k_B T_c)$. The pressure dependence of $R_\Delta$ is presented in the inset of Fig. 1(a). As we can see, the obtained results strongly deviate from the prediction of the BCS theory [21, 22], in which this dimensionless ratio is constant and equal to 3.53.

### 3.2 Condensation energy, thermodynamic critical field, and specific heat

Now we turn to a discussion of the temperature dependence of the condensation energy, thermodynamic critical field, and specific heat.

The difference between the normal state free energy and the superconducting state free energy in the absence of a magnetic field is called the condensation energy [$E_{\mathrm{cond}}(T) = F^N(T) - F^S(T)$]:

$$\frac{E_{\mathrm{cond}}(T)}{\rho(0)} = -\frac{2\pi}{\beta}\sum_{n=1}^{M}\left(\sqrt{\omega_n^2 + \Delta_n^2} - |\omega_n|\right) \times\left(Z_n^N\frac{|\omega_n|}{\sqrt{\omega_n^2 + \Delta_n^2}} - Z_n^S\right), \tag{5}$$

where $Z_n^N$ and $Z_n^S$ denote the mass renormalization

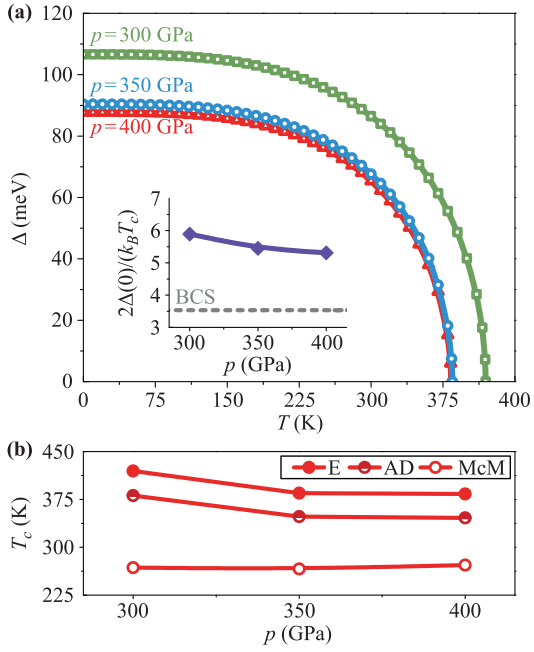


**Fig. 1** **(a)** The superconducting order parameter as a function of temperature. **(b)** The critical temperature as a function of pressure. The full circles denote results obtained using the Eliashberg formalism, the results presented by the half-filled circles and open circles are computed on the base of Allan–Dynes and McMillan analytical formulas, respectively. The inset presents zero-temperature gap to $T_c$ ratio vs. pressure.

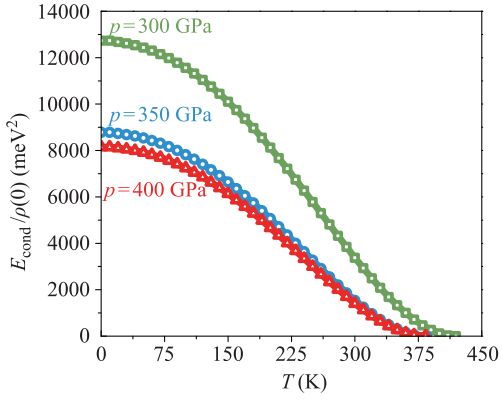


**Fig. 2** The condensation energy as a function of temperature.

functions for the normal and superconducting states, respectively. Moreover, $\rho(0)$ denotes the value of the electronic density of states at the Fermi level. In Fig. 2, we plot the condensation energy as a function of temperature.

The condensation energy is defined physically as the energy that stabilizes the superconducting state. Note, moreover, that for the zeroth temperature, the energy condensation is approximately equal to $\Delta^2$ and is related to the thermodynamic critical field ($H_c$) and to the specific heat difference between the superconducting and normal states ($\Delta C$) as follows:

$$\frac{H_C(T)}{\sqrt{\rho(0)}} = \sqrt{8\pi\left[\Delta F(T)/\rho(0)\right]} \tag{6}$$

and

$$\frac{\Delta C(T)}{k_B\rho(0)} = \frac{1}{\beta}\frac{\mathrm{d}^2\left[\Delta F(T)/\rho(0)\right]}{\mathrm{d}\left(k_BT\right)^2}. \tag{7}$$

The temperature dependence of the thermodynamic critical field is plotted in Fig. 3. Our result indicates that $H_c$ for $MgH_6$ takes the highest values at 300 GPa. At pressures between 350 and 400 GPa, the differences are slight in the entire temperature range. As in the case of the temperature dependence of the order parameter (Fig. 1) and condensation energy (Fig. 2), the thermodynamic critical field decreases with increasing temperature and vanishes at $T_c$.

In Fig. 4, we can trace the behavior of the specific heat difference between the superconducting and normal states as a function of temperature. The value of the characteristic specific heat jump at $T_c$ (marked by vertical dashed lines), like the value of the parameters presented above, decreases as the pressure grows.

The critical temperature, thermodynamic critical field, and specific heat functions obtained using the Eliashberg equations allowed us to estimate the dimensionless ratios $R_H \equiv T_cC^N(T_c)/H_c^2(0)$ and $R_c \equiv \Delta C(T_c)/C^N(T_c)$, where the specific heat for the normal state is defined as $C^N = \gamma T$, and $\gamma$ denotes the Sommerfeld constant: $\gamma \equiv (2/3)\pi^2\left(1+\lambda\right)k_B^2\rho(0)$. Note that, in the framework of the BCS theory, these ratios adopt universal values equal to 0.168 and 1.43, respectively [15]. For superconducting $MgH_6$, the obtained results disagree with the BCS prediction. In particular, $R_H$ is smaller than the BCS value, whereas $R_c$ greatly exceeds the BCS prediction. The obtained results as a function

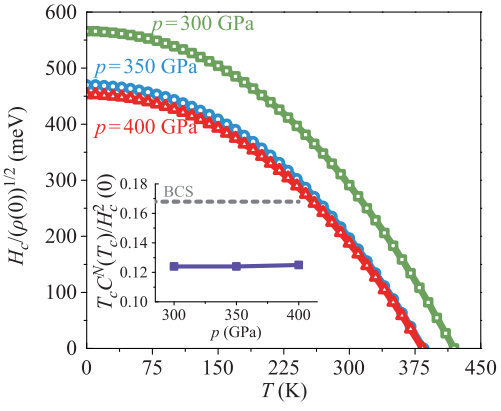


**Fig. 3** The thermodynamic critical field as a function of temperature. Inset presents the temperature dependencies of dimensionless ratio $T_cC^N(T_c)/H_c^2(0)$.

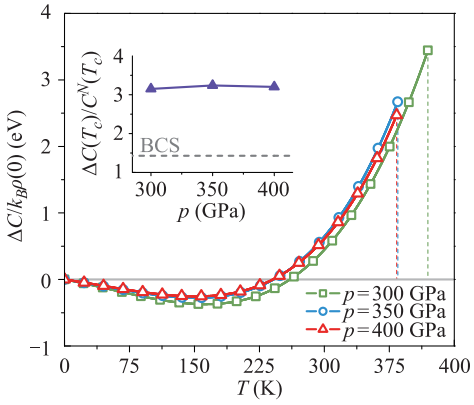


**Fig. 4** The specific heat difference between the superconducting and the normal state as a function of temperature. Inset presents the temperature dependencies of dimensionless ratio $\Delta C(T_c)/C^N(T_c)$.

of pressure are presented in the insets of Fig. 3 and Fig. 4. These discrepancies between the BCS prediction and the results of our numerical calculations arise from the existence of the strong-coupling and retardation effects in the system investigated. The Eliashberg theory goes beyond the BCS theory to include these effects, which enables it to describe the superconducting state quantitatively.

## 4 Conclusions

The thermodynamic properties of hydrogenated magnesium ($MgH_6$) at high pressures were investigated using the strong coupling Eliashberg theory of superconductivity. Our analysis show that the $T_c$ value of this superconductor significantly exceeds room temperature; in particular, $T_c$ increases from 384 to 420 K as the pressure decreases from 400 to 300 GPa. We observed similar behavior in other superconducting parameters such as the energy gap, specific heat, and thermodynamic critical field as a result of the strong coupling correlations. These parameters were used to estimate the dimensionless BCS ratios, which are not universal in the strong coupling limit. In particular, $R_\Delta \in \langle 5.89, 5.31\rangle$, $R_c \in \langle 3.15, 3.20\rangle$, and $R_H \in \langle 0.124, 0.125\rangle$, which correspond to the range of $p \in \langle 300, 400\rangle$ GPa. Non-BCS results have also been predicted [4, 23] and observed [7, 8] in hydrogen sulfide, so the results presented in this paper are expected to stimulate further experimental confirmation of the superconducting state in $MgH_6$.

**Acknowledgements** Authors would like to thank Guoying Gao (at Rice University) for scientific discussion and sharing the Eliashberg spectral functions.

## References

1. N. W. Ashcroft, Metallic hydrogen: A high-temperature superconductor? *Phys. Rev. Lett.* 21(26), 1748 (1968)
2. N. W. Ashcroft, Hydrogen dominant metallic alloys: High temperature superconductors? *Phys. Rev. Lett.* 92(18), 187002 (2004)
3. Y. Li, J. Hao, H. Liu, Y. Li, and Y. Ma, The metallization and superconductivity of dense hydrogen sulfide, *J. Chem. Phys.* 140(17), 174712 (2014)
4. A. P. Durajski, R. Szczęśniak, and L. Pietronero, High-temperature study of superconducting hydrogen and deuterium sulfide, *Ann. der Phys. (Berlin)*, 528, 358 (2016)
5. D. Duan, Y. Liu, F. Tian, D. Li, X. Huang, Z. Zhao, H. Yu, B. Liu, W. Tian, and T. Cui, Pressure-induced metallization of dense $(H_2S)_2H_2$ with high-$T_c$ superconductivity, *Sci. Rep.* 4, 6968 (2014)
6. R. Akashi, M. Kawamura, S. Tsuneyuki, Y. Nomura, and R. Arita, First-principles study of the pressure and crystal-structure dependences of the superconducting transition temperature in compressed sulfur hydrides, *Phys. Rev. B* 91(22), 224513 (2015)
7. A. Drozdov, M. I. Eremets, I. A. Troyan, V. Ksenofontov, and S. I. Shylin, Conventional superconductivity at 203 kelvin at high pressures in the sulfur hydride system, *Nature* 525(7567), 73 (2015)
8. M. Einaga, M. Sakata, T. Ishikawa, K. Shimizu, M. Eremets, A. Drozdov, I. Troyan, N. Hirao, and Y. Ohishi, Crystal structure of 200 K superconducting phase of sulfur hydride system, arXiv: 1509.03156 (2015)
9. H. Wang, J. S. Tse, K. Tanaka, T. Iitaka, and Y. Ma, Superconductive sodalite-like clathrate calcium hydride at high pressures, *Proc. Natl. Acad. Sci. USA* 109(17), 6463 (2012)
10. X. Feng, J. Zhang, G. Gao, H. Liu, and H. Wang, Compressed sodalite-like $MgH_6$ as a potential high-temperature superconductor, *RSC Adv.* 5, 59292 (2015)
11. G. Kresse and J. Furthmuller, Efficiency of ab-initio total energy calculations for metals and semiconductors using a plane-wave basis set, *Comput. Mater. Sci.* 6(1), 15 (1996)
12. J. P. Perdew, K. Burke, and M. Ernzerhof, Generalized gradient approximation made simple, *Phys. Rev. Lett.* 77(18), 3865 (1996)
13. G. Kresse and D. Joubert, From ultrasoft pseudopotentials to the projector augmented-wave method, *Phys. Rev. B* 59(3), 1758 (1999)
14. G. M. Eliashberg, Interactions between electrons and lattice vibrations in a superconductor, *Sov. Phys. JETP* 11, 696 (1960)
15. J. P. Carbotte, Properties of boson-exchange superconductors, *Rev. Mod. Phys.* 62(4), 1027 (1990)
16. R. Szczęśniak and T. P. Zemła, On the high-pressure superconducting phase in platinum hydride, *Supercond. Sci. Technol.* 28(8), 085018 (2015)

17. R. Szczęśniak, A. P. Durajski, and P. W. Pach, On the thermodynamic properties of the $Rb_3C_{60}$ superconductor, *Cryogenics* 61, 38 (2014)

18. R. Szczęśniak, A. P. Durajski, and L. Herok, Theoretical description of the $SrPt_3P$ superconductor in the strong-coupling limit, *Phys. Scr.* 89(12), 125701 (2014)

19. P. B. Allen and R. C. Dynes, Transition temperature of strong-coupled superconductors reanalyzed, *Phys. Rev. B* 905, 1975 (1975)

20. W. L. McMillan, Transition temperature of strong-coupled superconductors, *Phys. Rev.* 167(2), 331 (1968)

21. J. Bardeen, L. N. Cooper, and J. R. Schrieffer, Microscopic theory of superconductivity, *Phys. Rev.* 106(1), 162 (1957)

22. J. Bardeen, L. N. Cooper, and J. R. Schrieffer, Theory of superconductivity, *Phys. Rev.* 108(5), 1175 (1957)

23. A. P. Durajski, R. Szczęśniak, and Y. Li, Non-BCS thermodynamic properties of $H_2SH_2S$ superconductor, *Physica C* 515, 1 (2015)